

Luminescence Line Broadening of CdSe Nanoplatelets and Quantum Dots for Application in w-LEDs

Johanna C. van der Bok, Daphne M. Dekker, Matt L. J. Peerlings, Bastiaan B. V. Salzmann, and Andries Meijerink*

Cite This: *J. Phys. Chem. C* 2020, 124, 12153–12160

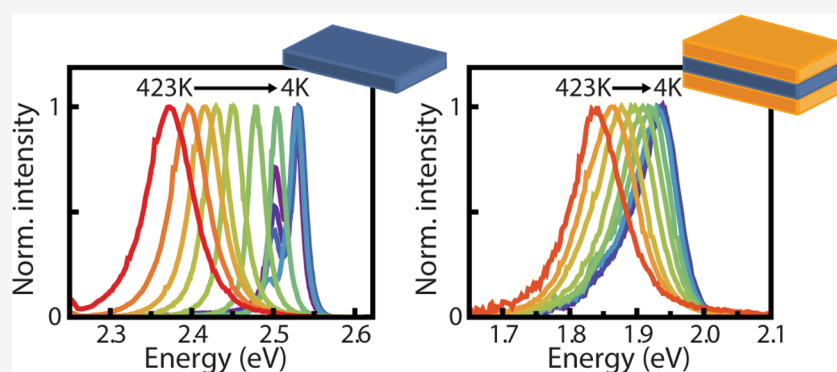
Read Online

ACCESS |

Metrics & More

Article Recommendations

Supporting Information



ABSTRACT: Nanoplatelets (NPLs) of CdSe are an emerging class of luminescent materials, combining tunable and narrow emission bands with high quantum yields. This is promising for application in white light LEDs (w-LEDs) and displays. The origin of the narrow spectral width of exciton emission in core NPL compared to core-shell NPL and quantum dot (QD) emission is not fully understood. Here we investigate and compare temperature-dependent emission spectra of core and core-shell CdSe NPLs and QDs. A wide temperature range, 4–423 K, is chosen to gain insight into contributions from homogeneous and inhomogeneous broadening and also to extend measurements into a temperature regime that is relevant for operating conditions in w-LEDs ($T \approx 423$ K). The results show that temperature-induced homogeneous broadening does not strongly vary between the various CdSe nanostructures ($\Delta E_{\text{hom}} \approx 60\text{--}80$ meV at 423 K) indicating that electron-phonon coupling strengths are similar. Only for the smallest QDs is stronger coupling observed. The origin of the narrow bandwidth reported at 300 K for core CdSe NPLs is attributed to a very narrow inhomogeneous line width. At 423 K, the spectral width of NPL exciton emission is still narrower than that of QDs. A comparison with traditional w-LED phosphors is made to outline advantages (tunability, narrow bandwidth, high efficiency) and disadvantages (color shift, stability issues) of NPLs for application in w-LEDs.

INTRODUCTION

In the past decade, a revolution in lighting has transformed the lighting market to a market dominated by white light LEDs (w-LEDs). The ban on incandescent lamps has contributed to this rapid transition. In addition, the high efficacy of w-LEDs (>100 lm/W), compactness, and long lifetime ($>30\,000$ h) make w-LEDs an attractive and flexible form of lighting in homes and offices and for outdoor illumination. The first generation of w-LEDs relied on generating white light from an efficient blue (In,Ga)N LED and partial blue-to-yellow conversion by the YAG:Ce phosphor. However, this design results in cold white light due to the lack of orange/red emission.¹ A remedy for the unpleasant cold color temperature was found by combining YAG:Ce with orange/red emitting phosphors. The most widely used phosphors nowadays rely on d-f emission from the lanthanide ions Eu^{2+} or Ce^{3+} and are characterized by relatively broad emission bands in the green, yellow, orange, or

red spectral region.¹ There is however a need for narrower band emitters to increase the efficacy of w-LEDs and improve the color gamut of LCD displays with w-LED backlights. Especially for the traditional red emitting phosphors, the broad emission band has a significant part of the emitted light in the wavelength region beyond 630 nm.² The sensitivity of the human eye drops sharply between 630 and 700 nm, thus making displays and w-LEDs less efficient (reduced lumen/W efficacy). Hence, there is a need for narrow band red emitters. This can be achieved by using semiconductor nanoparticles

Received: April 6, 2020

Revised: May 5, 2020

Published: May 6, 2020



(NPs) such as CdSe or InP quantum dots (QDs).^{3,4} The success of these NPs has already been demonstrated in the quantum dot light emitting diode (QLED) displays of Samsung.⁵ The use of both a narrow band green and red emitter increases the efficiency and widens the color gamut of these displays significantly. Still, there is a need for further reducing the spectral width.

A promising subclass of the semiconductor nanomaterials is CdSe nanoplatelets (NPLs) which exhibit an even narrower emission bandwidth compared to zero-dimensional (0D) QDs.⁶ The charge carriers in 2D NPLs are only confined in one dimension. Recent publications have reported on efficient visible emission from CdSe NPLs of only a few monolayers thick. The atomically well-defined nature of the thickness (typically 3.5 or 4.5 monolayers) minimizes inhomogeneous broadening, giving rise to narrow emission bands around 460 nm (3.5 monolayers) or 510 nm (4.5 monolayers).⁷ Full width at half maximum (fwhm) as narrow as ~ 40 meV⁸ has been reported at room temperature compared to ~ 70 – 120 meV for CdSe quantum dots.^{9–11} In order to increase the quantum yield and stability and to tune the photoluminescence (PL) toward the red, a CdS shell is grown around NPLs. However, upon introducing a shell the characteristic narrow bandwidth of CdSe NPLs is lost.¹² Contradictory explanations have been proposed for this increase in broadening. The broadening is either ascribed to stronger exciton phonon-coupling due the CdS shell¹³ or ascribed to an increase in inhomogeneous broadening caused by a no longer atomically well-defined NPL.¹⁴

Temperature-dependent studies can help to distinguish between the contributions of homogeneous and inhomogeneous broadening. Studies on thermal line broadening of CdSe NPL emission are typically limited to measurements up to room temperature.^{15,16} However, temperatures relevant for application in lamps and displays are much higher, even exceeding 150 °C in high power w-LEDs. At elevated temperatures, homogeneous broadening due to exciton–phonon coupling dominates over inhomogeneous broadening. It is therefore important to extend the temperature range and investigate the broadening of CdSe NPL and QD emission over a wide range of temperatures, up to 150 °C. The wider temperature range is not only relevant for practical applications but also extends the range in which thermal broadening can be investigated and compared to gain insight in differences between thermal broadening and exciton–phonon coupling in the different CdSe nanostructures. Finally, high-temperature measurements will allow for comparison of spectral widths for NPL emission and other luminescent materials used in w-LEDs (QDs, Mn⁴⁺- or Eu²⁺-phosphors) under relevant operation conditions to evaluate if NPLs still have a better performance at the elevated temperatures in w-LEDs.

In this report, we investigate and compare thermal exciton luminescence line broadening in a variety of CdSe nanostructures, viz., CdSe QDs and NPLs and CdSe/CdS core/shell QDs and NPLs. PL spectra were recorded and the PL bandwidths of QDs and NPLs of different sizes, and shell thicknesses were determined in a wide temperature regime, from 4 to 423 K (150 °C). The results show that homogeneous broadening is rather similar for the different types of CdSe nanomaterials and that the reduced emission bandwidth for core CdSe NPLs is caused by strongly reduced inhomogeneous broadening. Shell growth on NPLs gives rise to more inhomogeneous broadening and explains the increased

broadening of core–shell NPLs in comparison to core-only NPLs.

METHODS

CdSe Quantum dots were synthesized based on a method described by Li et al. using a reaction time of several seconds up to 10 min for the green (510QDs), orange (580QDs), and red (620QDs) emitting QDs, respectively.¹⁷ The number in the naming represents the emission wavelength at room temperature. 580QDs were passivated with two monolayers of CdS using the SILAR method.¹⁷ In the text, these are referred to as core–shell QDs. NPLs with a thickness of 3.5 monolayers (460NPLs) and 4.5 monolayers (510NPLs) were synthesized as published by Dubertret et al.¹⁸ The 510NPLs were passivated with a shell of one monolayer CdS using the c-ALD-method (1 ML core–shell NPLs) or six monolayers using a method developed by Rossinelli et al. (6 ML core–shell NPLs).^{19,20} Further details on the synthesis methods and transmission electron microscopy images are given in the Supporting Information.

The temperature-dependent measurements ranging from 4 to 423 K were performed in an Oxford Instruments liquid helium cryostat (up to 300 K) and a Linkam high-temperature stage (above 300 K) placed inside an Edinburgh FLS920 spectrometer equipped with a Hamamatsu R928 PMT detector and a 450 W xenon lamp as the excitation source. The excitation power used during the measurements was low, and an upper limit was estimated at ~ 100 mW/cm². At these low excitation powers, the line width is not affected by multiexciton emission. Emission of biexcitons is for example observed at an excitation power above 100 W/cm².²¹ To confirm this, emission spectra at higher excitation powers also were recorded, and no effect on the line width was observed (Figure S3).

The low-temperature measurements were performed in toluene or hexane for the QDs and NPLs, respectively. The particles were dispersed in the high boiling solvent 1-octadecene for high-temperature measurements. Emission spectra were corrected for the sensitivity of the detection system (emission monochromator throughput and detector response), and the intensity was converted to a photon flux per energy interval when the x -axis was converted to energy scale (from nm to eV).²²

RESULTS AND DISCUSSION

The spectral line width of emission from an ensemble of emitters is affected by inhomogeneous broadening and homogeneous broadening. Inhomogeneous broadening is caused by a variation in emission wavelength between different emitters, for example, due to size variations in the NPs. Inhomogeneous broadening is not strongly temperature dependent. Homogeneous broadening for exciton emission in QDs and NPLs is dominated by lifetime broadening. The Heisenberg uncertainty principle dictates that a shorter coherence lifetime of the excited and ground state gives rise to a larger uncertainty in the transition energy (emission wavelength). The main cause for a rapidly decreasing coherence lifetime upon heating is interaction with phonons (lattice vibrations). Phonon absorption, emission, and phonon scattering (Raman) processes contribute to a shortening of the coherence lifetime (dephasing time). The phonon-induced exciton dephasing processes are strongly temperature depend-

ent and are responsible for homogeneous line broadening of the exciton emission with temperature as the phonon population increases. The temperature dependence is complex as different types of phonon dephasing processes have a different temperature dependence.²³

Interaction with phonons also affects the position of the PL maximum. The shift of the PL maximum is influenced by various mechanisms, including phonon coupling and thermal expansion of the lattice. A phenomenological relation between the PL maximum and temperature was proposed by Varshni, including a T^2 -dependent term.²⁴ In order to extract a value for the exciton–phonon coupling strength and the effective phonon energy, the PL maximum as a function of the temperature can also be fitted with a semiempirical expression by Cardona et al.²⁵ The relation between the PL maximum and temperature is however not well understood. For example, the PL maxima of PbSe QDs as a function of the temperature can shift to lower energies, stay constant, or even shift to higher energies depending on the size of the QDs.²⁶ This makes the temperature shift of the PL maximum a less reliable probe for differences in exciton–phonon coupling strengths. Therefore, here we first evaluate differences in exciton–phonon coupling as well as the broadening at high temperatures by extracting the fwhm of the emission spectra over a broad range of temperatures.

The PL spectra of the investigated systems at temperatures ranging from 4 K (violet) to 423 K (red) are shown in Figure 1a–d and Figure S4a–d. An extra peak appeared on the low

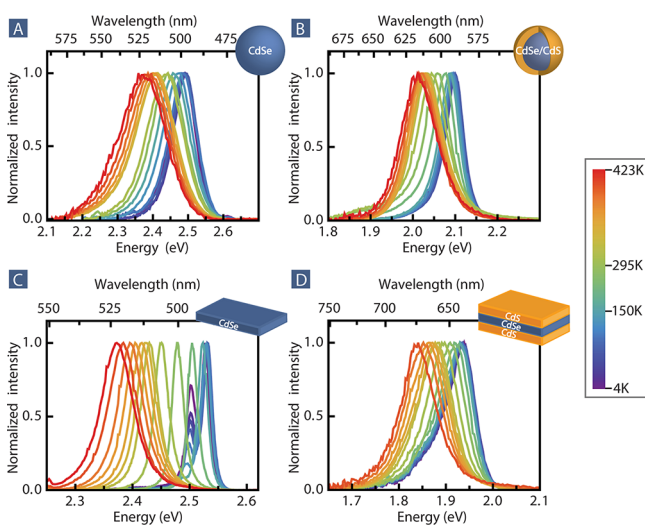


Figure 1. Normalized temperature-dependent spectra of (A) 510QDs, (B) core–shell QDs, (C) 510NPLs, and (D) 6 ML core–shell NPLs. Temperature ranges from 4 K (violet) to 423 K (red). At a temperature of 150 K and lower, a second peak is observed in C and a more asymmetric PL spectrum in D.

energy side upon cooling for the core NPLs (Figure 1c, Figure S4c and Figure S5). The origin of this low energy peak has been assigned to trion emission,²⁷ a phonon replica,²⁸ or excited state luminescence of a p-state.^{29,30} The higher energy peak is assigned to “normal” exciton emission, and from the PL spectra the fwhm of this higher energy peak was determined and used to investigate the exciton–phonon coupling strength. The splitting in two separate peaks is not observed for core–shell NPLs with one and six monolayers CdS, probably because of the larger inhomogeneous broadening. Interest-

ingly, the PL spectra of the core–shell NPLs do become more asymmetric at low temperatures, suggesting that also here the PL spectrum not only displays exciton emission below ~ 200 K, similar to what is observed for core NPLs. Recently, additional evidence supporting trion emission in core–shell NPLs has been reported.^{31,32}

The expected spectral line shape is Gaussian for inhomogeneous broadening and Lorentzian for homogeneous broadening.²³ The experimentally measured spectra could not be fitted well by either a Lorentzian or Gaussian over the entire temperature range. A product of a Lorentzian and Gaussian (approximation of a Voigt function³³) could be used to fit the data, but no trend was observed for the relative contribution of the Lorentzian component as a function of temperature. Therefore, the fwhm was determined directly by measuring the spectral width at half the peak intensity, except for the low-temperature spectra of the core and core–shell NPLs. To reduce interference by the lower energy emission, described in the previous paragraph, the width on the higher energy side was determined and taken as the hwhm for spectra recorded below 150 K and used to determine the fwhm.

The fwhm's obtained from the spectra in Figure 1 and Figure S4 are shown in Figure 2. The left-hand panel of Figure 2 shows the data for the NPLs, and the right-hand panel shows the data for the QDs. Note that the temperature is plotted from high to low temperature for the QDs in order to enable a better comparison of the fwhm at temperatures relevant for applications (423 K, where the two plots meet in the middle). Also note that the spectra at 423 K of the 6 ML core–shell NPLs were not taken into account, because the PL was irreversibly quenched (Figure S6).

Inhomogeneous Broadening. At 4 K, almost all phonons are frozen out, and phonon-induced dephasing processes are minimized. Therefore, the observed spectral width for ensemble measurements reflects the inhomogeneous broadening. The data in Figure 2 show that the inhomogeneous broadening for core NPLs of different thicknesses (3.5 or 4.5 monolayers) is similar and quite narrow (~ 18 meV). This reflects that the thickness of the core NPLs is indeed well-defined and the same within an ensemble of NPLs. The fwhm at 4 K significantly increases for the core–shell NPLs compared to the core-only NPLs, to ~ 60 meV. This suggests that the larger bandwidth for core–shell NPLs emission previously reported at room temperature is due to increased inhomogeneous broadening. This inhomogeneous broadening can be caused by inhomogeneities in shell thickness or defects at the core/shell interface. In addition, a clear red shift is observed upon CdS shell growth. The red shift is explained by electron delocalization over core and shell thus reducing the electron confinement energy. A larger (local) shell thickness on the NPL can lower the exciton energy and cause a redshift of the emission that depends on local variations in shell thickness.

The inhomogeneous broadening of the core QDs is larger than for the core NPLs and varies between 70 and 90 meV. No clear trend with size is observed. Inhomogeneous broadening is expected to become smaller when the size of the particle increases because a smaller size distribution is easier to achieve for larger particles, and size variations affect the emission energy less for larger QDs (weaker confinement effects). Indeed, less inhomogeneous broadening is observed for 610QDs, but 510QD and 580QD do not follow this trend and have a similar inhomogeneous line width. Variation in size distribution during synthesis may be the reason for not

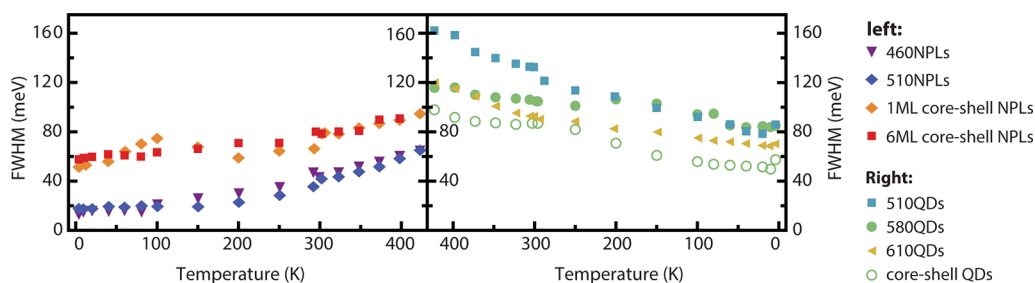


Figure 2. Temperature dependence of fwhm obtained from PL spectra in Figure 1 and Figure S4 (see text for details). Left panel: data NPLs: 460NPLs (purple triangles), 510NPLs (blue diamonds), 1 ML core-shell NPLs (orange diamonds), and 6 ML core-shell NPLs (red squares). Right panel, data of QDs: 510QDs (light blue squares), 580 QDs (green circles), 610QDs (yellow triangles), and core-shell QDs (open green circles). Data in the right panel are plotted from high to low temperature to allow for comparison of fwhm's at the operating temperature of w-LEDs at 423 K in the middle where the two plots meet.

observing the expected trend. An interesting observation can be done when the 580QDs and core-shell QDs are compared. The core-shell particles are synthesized using the 580QDs, but have a smaller fwhm at 4 K. The reduction in fwhm could be due to annealing of the core QDs when the mixture is heated up during the SILAR shell growth procedure. A smaller fwhm at room temperature upon shell growth was also observed by Bawendi et al., although a different synthesis method was used.⁹

Homogeneous Broadening. Upon raising the temperature, occupation of phonon modes reduces the coherence lifetime of the excited state through exciton-phonon coupling processes. This causes homogeneous broadening and therefore an increase of the line width as can be seen in Figure 2. At low temperatures, line broadening will be dominated by dephasing processes induced by coupling to low energy acoustic phonon modes. At higher temperatures when thermal occupation of higher energy optical phonon modes occurs, additional dephasing channels are opened, including higher-order, two-phonon processes (e.g., resonant and nonresonant Raman scattering). This can explain the steeper temperature dependence observed above 100 K.

The overall line width is a convolution of homogeneous and inhomogeneous broadening. It is therefore not correct to take the increase in fwhm for all NPs in Figure 2 as a measure for the exciton-phonon coupling strength. This is only possible when the inhomogeneous broadening is similar as is for example the case for 460NPLs and 510NPLs. The increase in fwhm as a function of the temperature is similar for these two systems, indicating similar exciton-phonon coupling in these systems. Typically, a stronger electron-phonon coupling is expected for stronger confinement, and this would give rise to a stronger coupling in the thinner 460NPLs.^{34,35} The fact that this is not observed may be related to the larger lateral dimensions of the 460NPLs compared to the 510NPLs; i.e., the 460NPLs do not have a smaller volume than the 510NPLs (Figure S2A,B). To confirm the influence of the lateral size on electron-phonon coupling, it will be interesting to conduct careful studies on line broadening in NPLs of the same thickness but with different lateral dimensions.

The exciton-phonon coupling strength can also be compared for the 580QDs and 510QDs, which also show a similar inhomogeneous broadening. Figure 2 shows that the exciton-phonon coupling is stronger in the smaller 510QDs. This is in agreement with the expectation that stronger confinement enhances the electron-phonon coupling strength.³⁵

To be able to compare the homogeneous broadening in all the different CdSe NPs (QDs and NPLs), deconvolution of the homogeneous and inhomogeneous broadening is needed. The experimentally measured fwhm (Γ_{total}) is a convolution of the homogeneous broadening which has a Lorentzian line shape and the inhomogeneous broadening which has a Gaussian line shape. The contribution of both line shapes results in a total broadening given by eq 1.³⁶ The inhomogeneous component ($\Gamma_{\text{Gaus/inhom}}$) is approximately the fwhm at 4 K.

$$\Gamma_{\text{total}} = \frac{\Gamma_{\text{Lor/hom}}}{2} + \sqrt{\frac{\Gamma_{\text{Lor/hom}}^2}{4} + \Gamma_{\text{Gaus/inhom}}^2} \quad (1)$$

Using eq 1 and the inhomogeneous line widths determined from the emission spectra at 4 K, the temperature dependence of the homogeneous line width was determined for the various CdSe core and core-shell nanostructures. The results are plotted in Figure 3 and show that the homogeneous

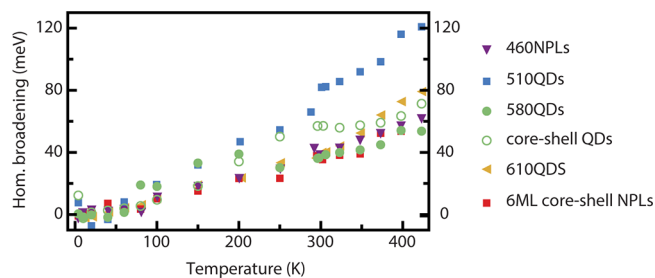


Figure 3. Temperature dependence of the homogeneous broadening for QDs and NPLs. The plot shows stronger homogeneous broadening for small NPs (510QDs, blue squares), but similar homogeneous broadening for the other investigated NPs at w-LED operating temperatures (423 K).

broadening is similar for the different CdSe nanostructures and increases to about 60–80 meV at 423 K. Only the 510 QDs show a stronger broadening (~ 120 meV at 423 K). Comparing the slopes for the homogeneous temperature broadening for the core-shell NPLs (red) and core NPLs (violet) reveals that the exciton-phonon coupling is not stronger in core-shell NPLs as was previously claimed. The same conclusion was also obtained by Achtstein et al. based on fitting the shift of the PL maximum.¹⁴ Nonetheless, no reduction in exciton-phonon coupling in core-shell NPLs is observed either, which deviates from results based on a shift of the PL maximum. The present measurements on fwhm over a

wide temperature range allow for a better comparison of the homogeneous line broadening than previous reports, which included measurements only up to 300 K¹⁴ or only from 300 to 370 K.³⁷ It is evident that especially between 300 and 423 K there is significant homogeneous broadening in a temperature regime where homogeneous broadening starts to dominate over inhomogeneous broadening. Within the experimental uncertainty, there is not a strong difference between the thermal broadening for the various QDs and NPLs investigated. The origin for the narrow bandwidth in core-only NPLs is clearly the extremely small inhomogeneous line width and not a weak electron–phonon coupling.

The exciton–phonon coupling strength can also be investigated by considering the temperature induced shift of the PL maximum. As discussed above, the peak shift is not only affected by exciton–phonon coupling, and this makes it a less reliable method to probe phonon-coupling strengths. Still, for the materials investigated the position of the PL maximum was determined for temperatures between 4 and 423 K as shown in Figure 4. The shift of the PL maximum in meV is given as well

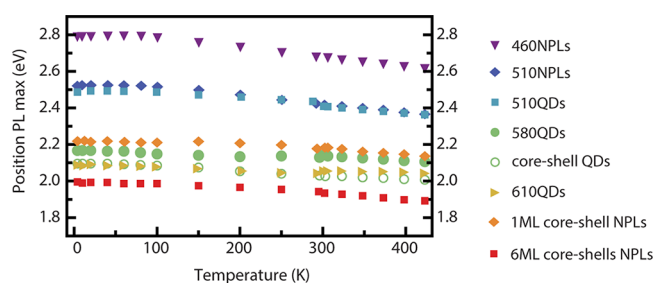


Figure 4. Temperature-dependent position PL maximum. Larger shifts of PL maximum are observed for NPLs compared to QDs.

as the relative shift. Larger temperature shifts are observed for the exciton emission in NPLs in comparison to QDs. Shell growth reduces the temperature induced shift of the exciton emission in the NPLs. For the QDs, a larger shift is observed for the smallest 510QDs. As discussed above, exciton–phonon coupling can alter the band structure, resulting in a shift of the PL maximum. Also lattice contraction upon lowering the temperature results in stronger confinement and gives rise to a blue shift of the PL maximum. The effect of the contraction of the lattice on the confinement is expected to be larger for more strongly confined systems resulting in a larger shift of the PL maximum. This is consistent with the observations in Figure 4, which shows a larger absolute temperature shift for 460NPLs than for the 510NPLs. When the relative shift is considered (see Table 1), both systems show a similar shift of ~6.2%. The temperature induced shift for core–shell NPLs is weaker with relative shifts of the exciton emission energy of ~3.8% and ~5.2% between 4 and 423 K. The relative shifts for exciton emission in QDs is smaller and varies between 2 and 5% with larger shifts observed for smaller QDs. One can speculate that the larger shifts observed in NPLs are connected with strong confinement in one direction that changes upon lattice expansion in this direction. It can be intuitively understood that this effect is stronger than expansion in all directions in a QD, but further (theoretical) investigations are needed to provide a full understanding of the temperature dependence of the exciton energy in NPLs and QDs and the role of lattice contraction and coupling to optical and acoustic phonon modes.

Table 1. Absolute and Relative Shift PL Maximum from 4 to 423 K^a

Material	Absolute shift (meV)	Relative shift (%)
▼ 460NPLs	175	6.2
◆ 510NPLs	157	6.2
■ 510QDs	127	5.1
● 580QDs	61	2.8
○ core-shell QDs	88	4.2
▶ 610QDs	47	2.3
◇ 1ML core-shell NPLs	81	3.8
■ 6ML core-shells NPLs	100	5.2

^aAbsolute shift (meV) and relative shift (%) of PL maximum over a temperature range of 4–423 K for materials shown in Figure 4.

Line Width and Line Shift at 423 K. Narrow band emission from CdSe NPLs has been suggested as a promising narrow band alternative for replacing CdSe and InP QDs in w-LEDs and displays. For color purity and widening the color gamut, a narrow band emission is desired, while for color point stability temperature induced shifts should be minimized.⁴ Most studies related to application of semiconductor NPLs and QDs as spectral converters in w-LEDs rely on measurements at room temperature.^{15,38} However, for on-chip application luminescent materials in w-LEDs, temperatures as high as 150 °C are reached. It is therefore important to consider spectral line widths and temperature-induced shifts at 150 °C for QDs and NPLs and compare these with traditional phosphors based on microcrystalline insulator materials doped with Eu²⁺, Ce³⁺, or Mn⁴⁺. Here we have extended the temperature range to this relevant temperature regime. When comparing the fwhm at 150 °C (423 K), it becomes evident that the core NPLs still outperform core–shell NPLs, QDs and core–shell QDs for applications due to the smaller fwhm of ~65 meV compared to 100–120 meV for core–shell NPLs and QDs. Especially when comparing the green emitting particles (510QDs and 510NPLs), it evident that NPLs have a fwhm that is a factor two smaller, making NPLs a superior candidate for a narrow green emitter in w-LEDs.

Core–shell NPLs, which emit in the red, have a slightly smaller or similar fwhm compared to the red emitting 610QDs (~120 meV at 423 K) and core–shell QDs (~100 meV at 423 K). In terms of fwhm, the core–shell NPLs do not underperform compared to QDs emitting in the red. Nevertheless, the spectral width of core–shell NPLs is larger compared to core-only NPLs and is related to the larger inhomogeneous width, as discussed above. Reducing the inhomogeneous broadening for core–shell NPLs is feasible by improving the synthesis procedure in order to obtain a better-defined and homogeneous shell thickness throughout the NPLs or a better-defined interface between the core and the shell. This will reduce the inhomogeneous broadening and make core–shell NPLs a better candidate for narrow red emitters. Rossinelli et al. have recently reported core–shell nanoplatelets with a narrower emission bandwidth.^{20,39} For application of red emitting NPLs in w-LEDs, the synthesis of stable NPLs with a high quantum yield and narrow band emission is crucial and improved shell-growth methods will be highly beneficial.

Finally, it is interesting to compare the performance at 423 K with traditional microcrystalline phosphors that are presently applied in w-LEDs such as (Ca,Sr)AlSiN₃:Eu²⁺ (CASN), SrLiAl₃N₄:Eu²⁺ (SLA), and K₂SiF₆:Mn⁴⁺ (KSF). The spectral width at low temperatures is much larger for the Eu²⁺ emission. Rather than a narrow zero-phonon line (which characterizes low temperature exciton emission in NPLs and QDs), a vibrationally broadened spectrum over typically 40–80 nm (120–235 meV) is observed, even for a single Eu²⁺ ion at 4 K. The thermal broadening is however less pronounced than for exciton emission and has a weak $\sqrt{\coth\left(\frac{h\omega}{kT}\right)}$ temperature dependence.^{23,40} Typical line widths for the red Eu²⁺ emission in CASN increase from 237 meV at 300 K to 251 meV at 423 K⁴¹ and from 182 meV (300 K) to 198 meV (423 K) for Eu²⁺ in SLA.⁴² Despite the weaker temperature dependence, it is evident that even at high temperatures the spectral widths of semiconductor nanostructures outperform that of traditional Eu²⁺ phosphors. The line emission of Mn⁴⁺ phosphors is narrower and concentrated in a number of sharp emission lines between 610 and 640 nm, spreading over a spectral region of only 90 meV, corresponding to an effective fwhm below 60 meV and thus competing with the narrow red emission of NPLs.⁴³

Temperature stability is an important characteristic of w-LED phosphors. Temperature-induced color shifts are undesired as a small shift of the emission maximum with temperature can give rise to noticeable color variations in w-LEDs. Color stability is therefore important to keep the color temperature of a w-LED independent of temperature fluctuations due to variations in the external temperature or operating conditions. The temperature shift of the emission maximum of NPL emission is relatively large. Between 300 and 423 K, a close to linear temperature shift is observed of 0.50 meV/K for 460 NPLs and 0.44 meV/K for 510 NPLs. For core–shell NPLs and QDs, the temperature shift of the emission maximum is smaller, but still significant (between 0.2 and 0.4 meV/K). In this respect, the shift of the emission maximum of traditional phosphors is much better (e.g., < 0.1 meV/K for SLA) and gives rise to better color temperature stability in response to external temperature variations. In addition to the thermal drift of the emission color, the stability and chemical integrity of CdSe NPs at the operating temperature in w-LEDs for on-chip application of QDs are a concern. Recently, coating strategies have been developed that allow for on-chip application in midpower LEDs^{3,44,45} and give hope that the stability of CdSe NPLs can be improved in a similar way to enable on-chip application in w-LEDs.

CONCLUSION

The spectral width and thermal broadening of exciton emission in core and core–shell CdSe NPLs has been investigated and compared with the temperature behavior of CdSe QDs in a wide temperature range (4–423 K), extending to temperatures relevant for application as spectral converters in w-LEDs. Measurements at cryogenic temperatures show that exciton emission of NPLs is characterized by a very narrow inhomogeneous line width (18 meV vs ~60–80 meV for QDs and core–shell NPLs). The narrow inhomogeneous broadening is attributed to the highly homogeneous (atomically precise) thickness of the NPLs of 3.5 (460 nm emission) or 4.5 monolayers (510 nm emission) of CdSe. Homogeneous (Heisenberg) broadening of exciton emission in NPLs and

QDs is due to phonon-assisted dephasing processes and increases strongly with temperature. At 4 K, homogeneous broadening is negligible as phonons are frozen out. The homogeneous line width increases rapidly with temperature, reaching widths varying between 60 and 80 meV at 423 K for different sizes of core and core–shell NPLs and QDs. Stronger phonon coupling seems to be observed for stronger confinement (smaller NPs), but the variation in homogeneous broadening is not large. Therefore, the size dependence of exciton phonon coupling cannot explain the much narrower bandwidth observed for CdSe NPLs. The narrow bandwidth for NPL exciton emission is therefore attributed to the narrow inhomogeneous line width and not to stronger exciton–phonon coupling in core–shell NPLs compared to core NPLs as previously suggested. In addition to line broadening, the temperature-induced shift of the exciton peak maximum was investigated. The thermal shift of the emission maximum for both NPLs and QDs is significantly larger than for traditional w-LED phosphors and may give rise to undesired fluctuations in the color temperature of w-LEDs. In spite of the large thermal shift and thermal stability issues at the operating temperature in w-LEDs, the favorable spectral properties make CdSe NPLs a promising class of materials for application in w-LEDs and displays.

ASSOCIATED CONTENT

Supporting Information

The Supporting Information is available free of charge at <https://pubs.acs.org/doi/10.1021/acs.jpcc.0c03048>.

Chemicals and detailed synthesis methods, TEM images, excitation power dependent spectra, temperature-dependent PL spectra of 580QDs, 610QDs, 460NPLs and 1 ML core–shell NPLs, low-temperature PL spectra of 510NPLs with Lorentzian fit, irreversible PL quenching of 6 ML core–shell NPLs (PDF)

AUTHOR INFORMATION

Corresponding Author

Andries Meijerink – Debye Institute of Nanomaterial Science, Utrecht University, Utrecht, The Netherlands; orcid.org/0000-0003-3573-9289; Email: a.meijerink@uu.nl

Authors

Johanna C. van der Bok – Debye Institute of Nanomaterial Science, Utrecht University, Utrecht, The Netherlands; orcid.org/0000-0002-1810-3513

Daphne M. Dekker – Debye Institute of Nanomaterial Science, Utrecht University, Utrecht, The Netherlands

Matt L. J. Peerlings – Debye Institute of Nanomaterial Science, Utrecht University, Utrecht, The Netherlands

Bastiaan B. V. Salzmann – Debye Institute of Nanomaterial Science, Utrecht University, Utrecht, The Netherlands

Complete contact information is available at: <https://pubs.acs.org/doi/10.1021/acs.jpcc.0c03048>

Notes

The authors declare no competing financial interest.

ACKNOWLEDGMENTS

We gratefully acknowledge NWO-CW (TopPunt Grant 718.015.002) for financial support.

REFERENCES

- (1) Chen, L.; Lin, C.-C.; Yeh, C.-W.; Liu, R.-S. Light Converting Inorganic Phosphors for White Light-Emitting Diodes. *Materials* **2010**, *3*, 2172–2195.
- (2) Stockman, A.; Sharpe, L. T. *Vision Res.* **2000**, *40*, 1711–1737.
- (3) Estrada, D.; Shimizu, K.; Bohmer, M.; Gangwal, S.; Diederich, T.; Grabowski, S.; Tashjian, G.; Chamberlin, D.; Shchekin, O. B.; Bhardwaj, J. 32–1: On-Chip Red Quantum Dots in White Leds for General Illumination. *Dig. Tech. Pap. - Soc. Inf. Disp. Int. Symp.* **2018**, *49*, 405–408.
- (4) Mangum, B. D.; Landes, T. S.; Theobald, B. R.; Kurtin, J. N. Exploring the Bounds of Narrow-Band Quantum Dot Downconverted Leds. *Photonics Res.* **2017**, *5*, A13–A22.
- (5) Jang, E.; Jang, H.; Kang, H. A.; Cho, O. 67–1: Invited Paper: Environmentally Friendly Quantum Dots for Display Applications. *Dig. Tech. Pap. - Soc. Inf. Disp. Int. Symp.* **2017**, *48*, 980–983.
- (6) Ithurria, S.; Dubertret, B. Quasi 2d Colloidal Cdse Platelets with Thicknesses Controlled at the Atomic Level. *J. Am. Chem. Soc.* **2008**, *130*, 16504–16505.
- (7) Ithurria, S.; Dubertret, B. *J. Am. Chem. Soc.* **2008**, *130*, 16504–16505.
- (8) Tessier, M. D.; Javaux, C.; Maksimovic, I.; Lorientte, V.; Dubertret, B. Spectroscopy of Single Cdse Nanoplatelets. *ACS Nano* **2012**, *6*, 6751–6758.
- (9) Chen, O.; Zhao, J.; Chauhan, V. P.; Cui, J.; Wong, C.; Harris, D. K.; Wei, H.; Han, H.-S.; Fukumura, D.; Jain, R. K.; et al. Compact High-Quality Cdse–Cds Core–Shell Nanocrystals with Narrow Emission Linewidths and Suppressed Blinking. *Nat. Mater.* **2013**, *12*, 445–451.
- (10) Reiss, P.; Carayon, S.; Bleuse, J.; Pron, A. Low Polydispersity Core/Shell Nanocrystals of Cdse/Znse and Cdse/Znse/Zns Type: Preparation and Optical Studies. *Synth. Met.* **2003**, *139*, 649–652.
- (11) Cui, J.; Beyler, A. P.; Marshall, L. F.; Chen, O.; Harris, D. K.; Wanger, D. D.; Brokmann, X.; Bawendi, M. G. Direct Probe of Spectral Inhomogeneity Reveals Synthetic Tunability of Single-Nanocrystal Spectral Linewidths. *Nat. Chem.* **2013**, *5*, 602–606.
- (12) Mahler, B.; Nadal, B.; Bouet, C.; Patriarche, G.; Dubertret, B. *J. Am. Chem. Soc.* **2012**, *134*, 18591–18598.
- (13) Tessier, M. D.; Mahler, B.; Nadal, B.; Heuclin, H.; Pedetti, S.; Dubertret, B. Spectroscopy of Colloidal Semiconductor Core/Shell Nanoplatelets with High Quantum Yield. *Nano Lett.* **2013**, *13*, 3321–3328.
- (14) Achtstein, A. W.; Marquardt, O.; Scott, R.; Ibrahim, M.; Riedl, T.; Prudnikau, A. V.; Antanovich, A.; Owschimikow, N.; Lindner, J. K. N.; Artemyev, M.; et al. Impact of Shell Growth on Recombination Dynamics and Exciton–Phonon Interaction in Cdse–Cds Core–Shell Nanoplatelets. *ACS Nano* **2018**, *12*, 9476–9483.
- (15) Scott, R.; Prudnikau, A. V.; Antanovich, A.; Christodoulou, S.; Riedl, T.; Bertrand, G. H. V.; Owschimikow, N.; Lindner, J. K. N.; Hens, Z.; Moreels, I.; et al. A Comparative Study Demonstrates Strong Size Tunability of Carrier-Phonon Coupling in Cdse-Based 2d and 0d Nanocrystals. *Nanoscale* **2019**, *11*, 3958–3967.
- (16) Achtstein, A. W.; Schliwa, A.; Prudnikau, A.; Hardzei, M.; Artemyev, M. V.; Thomsen, C.; Woggon, U. Electronic Structure and Exciton-Phonon Interaction in Two-Dimensional Colloidal Cdse Nanosheets. *Nano Lett.* **2012**, *12*, 3151–3157.
- (17) Li, J. J.; Wang, Y. A.; Guo, W.; Keay, J. C.; Mishima, T. D.; Johnson, M. B.; Peng, X. Large-Scale Synthesis of Nearly Monodisperse Cdse/Cds Core/Shell Nanocrystals Using Air-Stable Reagents Via Successive Ion Layer Adsorption and Reaction. *J. Am. Chem. Soc.* **2003**, *125*, 12567–12575.
- (18) Ithurria, S.; Bousquet, G.; Dubertret, B. Continuous Transition from 3d to 1d Confinement Observed During the Formation of Cdse Nanoplatelets. *J. Am. Chem. Soc.* **2011**, *133*, 3070–3077.
- (19) Ithurria, S.; Talapin, D. V. *J. Am. Chem. Soc.* **2012**, *134*, 18585–18590.
- (20) Rossinelli, A. A.; Riedinger, A.; Marqués-Gallego, P.; Knüsel, P. N.; Antolinez, F. V.; Norris, D. J. High-Temperature Growth of Thick-Shell Cdse/Cds Core/Shell Nanoplatelets. *Chem. Commun.* **2017**, *53*, 9938–9941.
- (21) Htoon, H.; Malko, A. V.; Bussian, D.; Vela, J.; Chen, Y.; Hollingsworth, J. A.; Klimov, V. I. Highly Emissive Multiexcitons in Steady-State Photoluminescence of Individual “Giant” Cdse/Cds Core/Shell Nanocrystals. *Nano Lett.* **2010**, *10*, 2401–2407.
- (22) Mooney, J.; Kambhampati, P. Get the Basics Right: Jacobian Conversion of Wavelength and Energy Scales for Quantitative Analysis of Emission Spectra. *J. Phys. Chem. Lett.* **2013**, *4*, 3316–3318.
- (23) Henderson, B.; Imbusch, G. F. *Optical Spectroscopy of Inorganic Solids*; Clarendon Press, 2006; pp 199–238.
- (24) Varshni, Y. P. Temperature Dependence of the Energy Gap in Semiconductors. *Physica* **1967**, *34*, 149–154.
- (25) Logothetidis, S.; Cardona, M.; Lautenschlager, P.; Garriga, M. *Phys. Rev. B: Condens. Matter Mater. Phys.* **1986**, *34*, 2458–2469.
- (26) Dey, P.; Paul, J.; Bylisma, J.; Karaiskaj, D.; Luther, J. M.; Beard, M. C.; Romero, A. H. *Solid State Commun.* **2013**, *165*, 49–54.
- (27) Shornikova, E. V.; Biadala, L.; Yakovlev, D. R.; Sapega, V. F.; Kusrayev, Y. G.; Mitioglu, A. A.; Ballottin, M. V.; Christianen, P. C. M.; Belykh, V. V.; Kochiev, M. V.; et al. Addressing the Exciton Fine Structure in Colloidal Nanocrystals: The Case of Cdse Nanoplatelets. *Nanoscale* **2018**, *10*, 646–656.
- (28) Biadala, L.; Liu, F.; Tessier, M. D.; Yakovlev, D. R.; Dubertret, B.; Bayer, M. *Nano Lett.* **2014**, *14*, 1134–1139.
- (29) Achtstein, A. W.; Scott, R.; Kickhöfel, S.; Jagsch, S. T.; Christodoulou, S.; Bertrand, G. H. V.; Prudnikau, A. V.; Antanovich, A.; Artemyev, M.; Moreels, I. P-State Luminescence in Cdse Nanoplatelets: Role of Lateral Confinement and a Longitudinal Optical Phonon Bottleneck. *Phys. Rev. Lett.* **2016**, *116*, DOI: 10.1103/PhysRevLett.116.116802.
- (30) Specht, J. F.; Scott, R.; Corona Castro, M.; Christodoulou, S.; Bertrand, G. H. V.; Prudnikau, A. V.; Antanovich, A.; Siebbeles, L. D. A.; Owschimikow, N.; Moreels, I.; et al. Size-Dependent Exciton Substructure in Cdse Nanoplatelets and Its Relation to Photoluminescence Dynamics. *Nanoscale* **2019**, *11*, 12230–12241.
- (31) Antolinez, F. V.; Rabouw, F. T.; Rossinelli, A. A.; Cui, J.; Norris, D. J. Observation of Electron Shakeup in Cdse/Cds Core/Shell Nanoplatelets. *Nano Lett.* **2019**, *19*, 8495–8502.
- (32) Shornikova, E. V.; Biadala, L.; Yakovlev, D. R.; Feng, D.; Sapega, V. F.; Flipo, N.; Golovatenko, A. A.; Semina, M. A.; Rodina, A. V.; Mitioglu, A. A.; et al. Electron and Hole G-Factors and Spin Dynamics of Negatively Charged Excitons in Cdse/Cds Colloidal Nanoplatelets with Thick Shells. *Nano Lett.* **2018**, *18*, 373–380.
- (33) Jain, V.; Biesinger, M. C.; Linford, M. R. The Gaussian-Lorentzian Sum, Product, and Convolution (Voigt) Functions in the Context of Peak Fitting X-Ray Photoelectron Spectroscopy (Xps) Narrow Scans. *Appl. Surf. Sci.* **2018**, *447*, 548–553.
- (34) Mittleman, D. M.; Schoenlein, R. W.; Shiang, J. J.; Colvin, V. L.; Alivisatos, A. P.; Shank, C. V. Quantum Size Dependence of Femtosecond Electronic Dephasing and Vibrational Dynamics in Cdse Nanocrystals. *Phys. Rev. B: Condens. Matter Mater. Phys.* **1994**, *49*, 14435–14447.
- (35) Takagahara, T. *Electron-Phonon Interactions in Semiconductor Quantum Dots*; Springer: Berlin, Heidelberg, 2002; pp 115–147.
- (36) Olivero, J. J.; Longbothum, R. L. Empirical Fits to the Voigt Line Width: A Brief Review. *J. Quant. Spectrosc. Radiat. Transfer* **1977**, *17*, 233–236.
- (37) Bose, S.; Shendre, S.; Song, Z.; Sharma, V. K.; Zhang, D. H.; Dang, C.; Fan, W.; Demir, H. V. Temperature-Dependent Optoelectronic Properties of Quasi-2d Colloidal Cadmium Selenide Nanoplatelets. *Nanoscale* **2017**, *9*, 6595–6605.
- (38) Osinski, J.; Kurtin, J. N.; Mangum, B. D.; Nelson, R. Multiple Quantum Dot (Qd) Device. US9,423,083B2, March 7, 2014.
- (39) Rossinelli, A. A.; Rojo, H.; Mule, A. S.; Aellen, M.; Cocina, A.; De Leo, E.; Schaublin, R.; Norris, D. J. Compositional Grading for Efficient and Narrowband Emission in Cdse-Based Core/Shell Nanoplatelets. *Chem. Mater.* **2019**, *31*, 9567–9578.
- (40) ten Kate, O. M.; Zhang, Z.; van Ommen, J. R.; Hintzen, H. T. Dependence of the Photoluminescence Properties of Eu²⁺ Doped

M–Si–N (M = Alkali, Alkaline Earth or Rare Earth Metal) Nitridosilicates on Their Structure and Composition. *J. Mater. Chem. C* **2018**, *6*, 5671–5683.

(41) Tian, J.; Zhuang, W.; Liu, R.; Wang, L.; Liu, Y.; Yan, C.; Chen, G.; Xu, H.; Chen, M.; Jiang, Z.; et al. Enhanced Thermal Quenching Characteristic Via Carbon Doping in Red-Emitting CaAl₂Si₂O₇:Eu²⁺ Phosphors. *J. Am. Ceram. Soc.* **2019**, *102*, 7336–7346.

(42) Zhang, X.; Tsai, Y. T.; Wu, S. M.; Lin, Y. C.; Lee, J. F.; Sheu, H. S.; Cheng, B. M.; Liu, R. S. Facile Atmospheric Pressure Synthesis of High Thermal Stability and Narrow-Band Red-Emitting SrAl₂Si₂O₇:Eu²⁺ Phosphor for High Color Rendering Index White Light-Emitting Diodes. *ACS Appl. Mater. Interfaces* **2016**, *8*, 19612–19617.

(43) Senden, T.; Van Harten, E. J.; Meijerink, A. Synthesis and Narrow Red Luminescence of Cs₂Na₂Si₂O₇:Mn⁴⁺, a New Phosphor for Warm White Leds. *J. Lumin.* **2018**, *194*, 131–138.

(44) Haley, K. N.; Mangum, B. D.; Zhao, W.; Stott, N. E.; Kurtin, J. N. Quantum Dot (Qd) Polymer Composites for on-Chip Light Emitting Diode (Led) Applications. US2018/0006195A1, September 19, 2017.

(45) Zhao, W.; Kurtin, J. N. Composition of, and Method for Forming, a Semiconductor Structure with Multiple Insulator Coatings. US10,266,760B2, April 23, 2019.